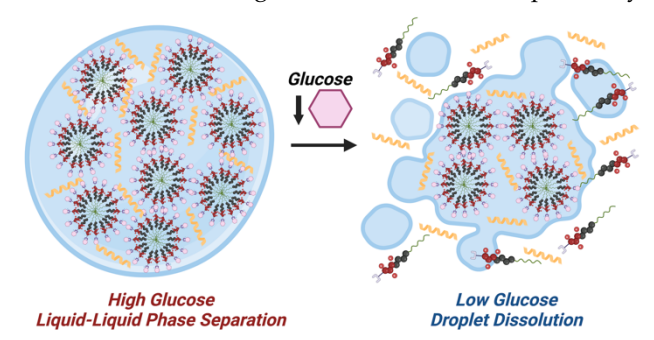
# Glucose-Driven Droplet Formation in Complexes of a Supramolecular Peptide and Therapeutic Protein

Sihan Yu,<sup>1</sup> Weike Chen,<sup>1</sup> Guoqiang Liu,<sup>2</sup> Belen Flores,<sup>1</sup> Emily L. DeWolf,<sup>1</sup> Bowen Fan,<sup>1</sup> Yuanhui Xiang,<sup>1</sup> and Matthew J. Webber<sup>1,\*</sup>

- 1- University of Notre Dame, Department of Chemical & Biomolecular Engineering, Notre Dame, IN 46556 USA
- 2- University of Notre Dame, Integrated Biomedical Sciences Program, Notre Dame, IN 46556 USA
- \*- mwebber@nd.edu

ABSTRACT: Biology achieves remarkable function through processes arising from spontaneous or transient liquid-liquid phase separation (LLPS) of proteins and other biomolecules. While polymeric systems can achieve similar phenomena through simple or complex coacervation, LLPS with supramolecular materials has been less commonly shown. Functional applications for synthetic LLPS systems are an expanding area of emphasis, with particular focus on capturing the transient and dynamic state of these structures for use in biomedicine. Here, a net-cationic supramolecular peptide amphiphile building block with a glucose-binding motif is shown that forms LLPS structures when combined with a net-negatively charged therapeutic protein, dasiglucagon, in the presence of glucose. The droplets that arise are dynamic and coalesce quickly. However, the interface can be stabilized by addition of a 4-arm star PEG. When the stabilized droplets formed in glucose are transferred to a bulk phase containing different glucose concentrations, their stability and lifetime decreases according to bulk glucose concentration. This glucose-dependent formation translates into accelerated release of dasiglucagon in the absence of glucose; this hormone analogue itself functions therapeutically

to correct low blood glucose (hypoglycemia). These droplets also offer function in mitigating the most severe effects of hypoglycemia arising from an insulin overdose through delivery of dasiglucagon in a mouse model of hypoglycemic rescue. Accordingly, this approach to use complexation between a supramolecular peptide amphiphile and a therapeutic protein in the presence of glucose leads to droplets with functional potential to dissipate for the release of the therapeutic in low blood glucose environments.



KEYWORDS: Supramolecular Chemistry; Dynamic-Covalent Chemistry; Biomaterials; Self-Assembly; Drug Delivery

## 1. INTRODUCTION

Liquid-liquid phase separation (LLPS) of biopolymers has been increasingly found to play central roles in an assortment of biological processes.<sup>1,2</sup> One example is in membraneless organelles, spontaneous assemblies within cells that lack a lipid bilayer and are driven by LLPS of proteins and other biomolecules to form liquid- or gel-like states.<sup>3</sup> The localized concentration of biomolecules within LLPS structures, such as in the nucleolus, histone loci, Cajal bodies, and stress granules, serve key functional and biocatalytic roles in cell biology, regulating cellular gene expression, proliferation, and

differentiation.<sup>4</sup> Various of these roles have even been recreated by artificial engineering of membraneless organelles within cells to enable unnatural functionalities.<sup>5,6</sup> LLPS is also a common phenomenon observed in polymeric macromolecules, a process often known as coacervation.<sup>7</sup> Polymer coacervates have been applied as model systems of membraneless organelles,<sup>8,9</sup> used as responsive carries for the delivery of therapeutics,<sup>10</sup> and explored for a variety of biomedical applications.<sup>11</sup>

Supramolecular polymers are an expanding class of materials that capture many of the physical traits of

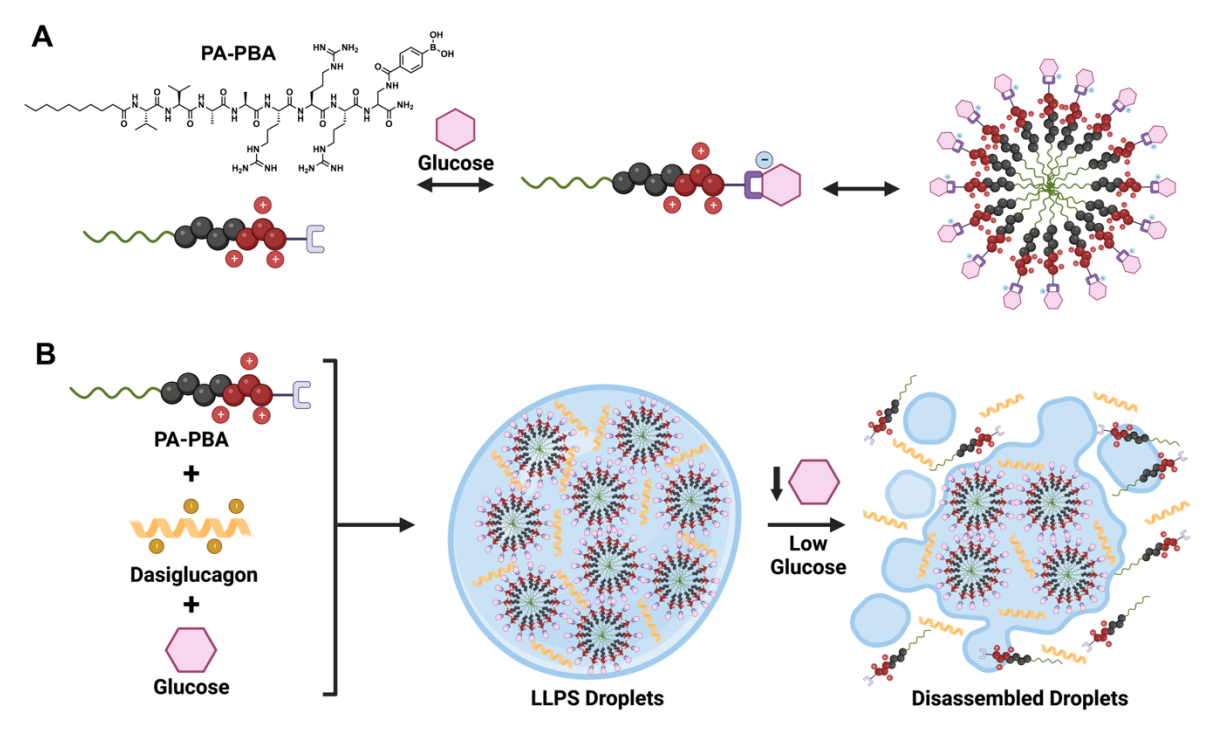


**Figure 1:** (A) The molecular structure of PA-PBA, comprising a peptide amphiphile of sequence  $C_{10}$ - $V_2A_2R_3$ Dap(PBA) wherein a phenylboronic acid (PBA) motif is presented for glucose binding. Glucose-bound PA-PBA self-assembles into spherical structures. (B) When the net-positive PA-PBA is mixed with the net-negative dasiglucagon therapeutic in the presence of glucose, droplets form via liquid-liquid phase separation (LLPS). The formed droplets dissolve when introduced into conditions of low glucose, releasing dasiglucagon.

covalent macromolecules, forming high persistence from non-covalent monomer structures assemblies.<sup>12</sup> One such class of supramolecular polymers that has been extensively studied is the peptide amphiphile (PA), which can form high aspect-ratio assemblies by leveraging a combination of hydrophobic association of prosthetic alkyl groups with peptidedriven hydrogen bonding.13,14 PAs have been explored in the context of biomaterials for a number of biomedical applications.<sup>15,16</sup> However, whereas the biopolymers that offer bio-inspiration for PA-based supramolecular polymers, including peptide-based materials and amyloid assemblies, 17,18 readily participate in LLPS, PAs have not been observed to exhibit LLPS phenomena. Moreover, the observation of LLPS is curiously uncommon in the broader field of supramolecular polymers, in spite of countless examples of this phenomenon in their covalent macromolecular counterparts.

Here, a PA bearing a phenylboronic acid (PBA) is explored in conjunction with a therapeutic glucagon analogue (dasiglucagon) for glucose-directed LLPS (*Fig 1*). PBAs are Lewis acids that have been frequently explored as synthetic glucose sensors in material design due to their ability to form dynamic-covalent bonds with glucose and related diols.<sup>19</sup> Interestingly, when the netpositive PA is combined with the net-negative

dasiglucagon protein in the presence of glucose, a droplet phase emerges comprised of both PA and protein (*Fig* 1B). These droplets are dynamic and readily coalesce, though interfacial stabilization using another polymer improves stability. Furthermore, the dependence of droplet formation on the presence of glucose to modulate PA electrostatics results in their dissolution under conditions of low glucose, leading to release of a dasiglucagon payload that itself is the therapeutic remedy for low blood glucose. Accordingly, dasiglucagon release from the droplets is accelerated in the absence of glucose, offering a functional strategy to mitigate the severity of hypoglycemia in a rodent model of insulin overdose.

#### 2. RESULTS & DISCUSSION

2.1 Molecular Design. The classical PA motif consists of a saturated alkyl chain providing a hydrophobic driving force for self-assembly and micellization in water that is covalently attached to the terminus of a peptide comprising at least two domains: a fibrilizing domain promoting parallel intermolecular  $\beta$ -sheet formation for directional hydrogen bonding and one-dimensional assembly, and a charged headgroup facilitating solubility and favorable solvent interactions on the micelle surface. Further, the surface of the resulting nanostructures enables high-density presentation of bioactive signals to recreate functions and structures of

native extracellular matrix, with uses in an assortment of biomedical applications.<sup>21</sup> In an initial effort that was intended to make glucose-responsive hydrogels, here a PA was designed for surface-presentation of an amidelinked PBA motif. The sequence of the specific PA studied (PA-PBA) was  $C_{10}$ – $V_2A_2R_3$ -Dap(PBA) (Fig 1A). The  $C_{10}$ saturated alkyl segment was selected to reduce the hydrophobic driving force for self-assembly so as to enhance the eventual glucose-responsiveness of the system, and followed a design from prior work exploring enzymatically driven PA hydrogelation.<sup>22</sup> Similarly, an established short  $\beta$ -sheet sequence of two valine residues followed by two alanine residues (V2A2) was also inserted with the intention to promote peptide hydrogelation while at the same time not having the same high cohesive interactions of traditionally longer β-sheet segments. A segment of three arginines (R3) offered a hydrophilic head group to promote solubility and order self-assembly of the molecule in water. On the C-terminal end of the molecule opposite the alkyl tail, a diaminopropionic acid (Dap) residue was included; synthetically this was inserted on-resin with its β-amine protected with a 4methyltrityl (Mtt) protecting group, for selective on-resin deprotection using mild acidic conditions to enable sidechain functionalization with a PBA motif through amide bond formation. This amide-linked PBA would be expected to have a  $pK_a$  of ~8.4;<sup>23</sup> this would not typically lead to a significant amount of the tetrahedral boronate species necessary for glucose binding under physiological conditions. However, the positioning of this PBA next to cationic arginine residues was expected to significantly reduce its effective  $pK_a$ , a phenomenon also observed in PBA-modified cationic polymers.<sup>24,25</sup>

The design of PA-PBA was initially intended for a goal of glucose-directed hydrogelation. Specifically, glucose binding to a PBA group at pH conditions near to its  $pK_a$  is known to shift the equilibrium to the negatively charged tetrahedral boronate ester species.<sup>19</sup> As such, in the presence of glucose, the PBA group on the molecule should become more negatively charged, in turn reducing the net charge on the PA-PBA headgroup. The reduced electrostatic repulsion upon glucose binding would then be expected to enhance self-assembly and hydrogelation, as is also seen for other PA designs upon introduction of charge-screening ionic species or changes in pH.<sup>26,27</sup> As an alternative to a prior report exploring enzymatically driven hydrogelation in the presence of glucose through the actuation of xenogeneic glucose oxidase,<sup>22</sup> the current approach envisioned with PA-PBA was thought to offer a more biocompatible and direct way to achieve a glucose-stabilized hydrogel for release of glucagon upon hypoglycemia. PBA-modified oligopeptides were previously shown to self-assemble into nanocoils that then became entangled into a hydrogel network upon PBA–glucose binding. <sup>28</sup> However, initial efforts with the platform here failed to realize formation of a self-supporting hydrogel upon addition of glucose. TEM of PA-PBA in its glucose-bound state instead revealed formation of spherical micellar structures (Fig S1), likely explaining the inability of this molecule to form the nanofibrillar hydrogels of a typical PA material. Accordingly, cohesive interactions in this relatively short  $\beta$ -sheet segment were not sufficient to overcome the electrostatic repulsion and hydrated volume of its charged and glucose-bound headgroup.

2.2 Observation of Droplet Formation. Here, a stabilized and water-soluble glucagon analogue, dasiglucagon,29 was explored for formulation and delivery with PA-PBA. It was initially reasoned that though PA-PBA did not gel on its own, the added electrostatic screening from the negatively charged dasiglucagon could contribute to nanofibril formation and hydrogelation of PA-PBA, as had been shown for other arginine-rich cationic PAs when mixed with negatively charged biomolecules.30,31 Upon mixing PA-PBA at 2 mg/mL with synthesized dasiglucagon at 0.2 mg/mL in glucose conditions of 200 mg/dL resembling a glucose concentration on the high end of the normal physiological range, the resulting mixture appeared cloudy, having the appearance of a colloidal suspension rather than a self-supporting hydrogel. To further probe this phenomenon, the components were mixed under different glucose concentrations ranging from 0-200 mg/dL and sample turbidity was monitored in real time (Fig 2A) by measuring absorbance (*i.e.*, light scattering) at  $\lambda$ =600 nm, where the individual components have negligible molecular absorbance. These data point to a rapid increase in sample turbidity shown by greater overall light scattering in samples prepared at higher glucose concentrations, whereas samples remained translucent at low glucose concentrations (Fig 2B). Optical microscopy of these samples revealed the presence of spherical droplets, with the number generally increasing with increases in glucose concentration of the mixture (Fig 2C). Zeta potential measurements were collected to study the charge state of PA-PBA at 2 mg/mL across a range of different glucose concentrations (Fig S2). These data show a steady reduction in the zeta potential of PA-PBA as glucose level is increased, from  $34.1 \pm 1.7$  mV at 0 mg/dL glucose to  $18.9 \pm 1.7$  mV at 200 mg/dL. Comparatively, dasiglucagon at 0.2 mg/mL had a zeta potential of -19.9 ± 0.3 mV. Accordingly, as PA-PBA binds to glucose, the charged tetrahedral boronate of its PBA motif is stabilized, as expected,19 leading to a reduction in the overall extent of positive charge of the PA-PBA. Interestingly, at these higher glucose levels the charge of

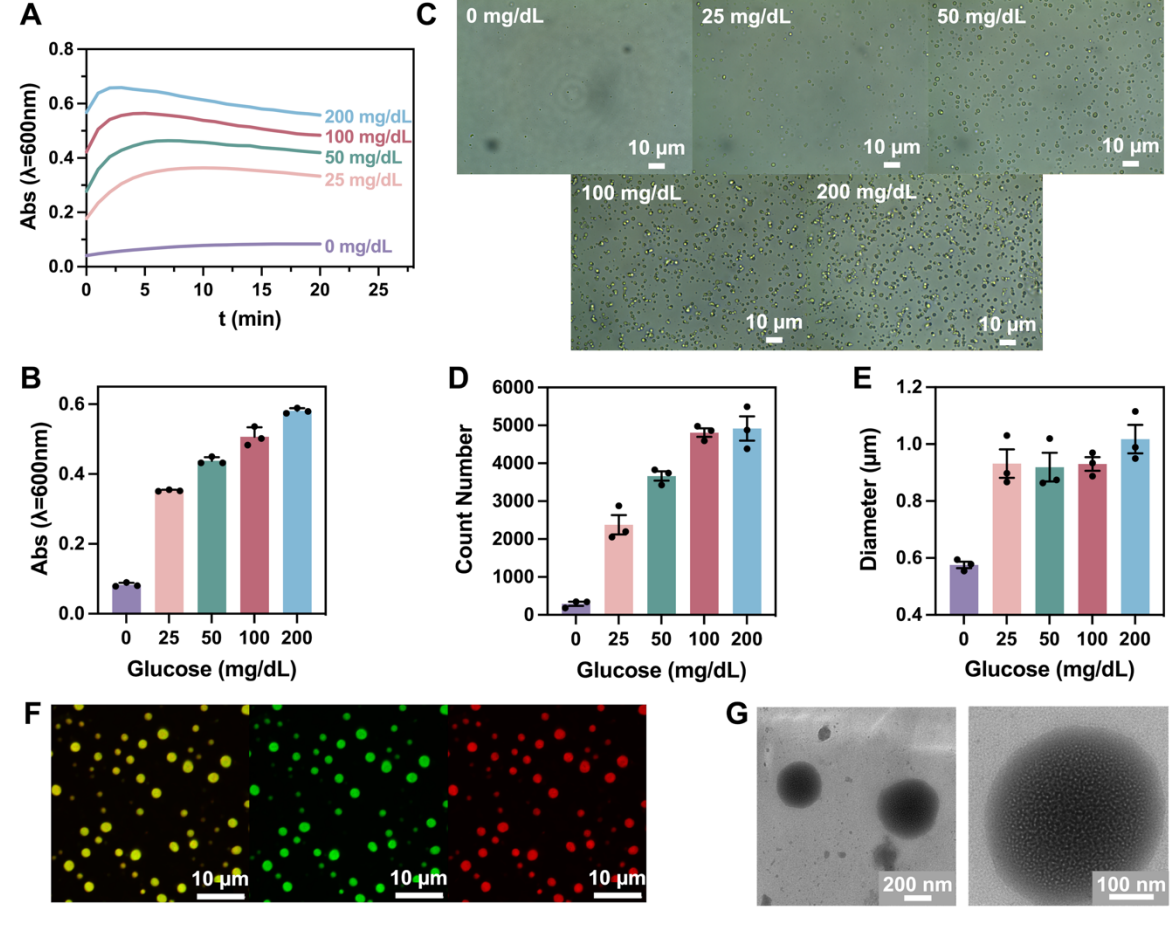


**Figure 2:** (**A**) Turbidity ( $\lambda$ =600 nm) measured over time after mixing PA-PBA, dasiglucagon, and different concentrations of glucose. (**B**) Quantification of turbidity ( $\lambda$ =600 nm) for samples prepared at different glucose concentrations at 15 min after mixing (n=3/group,  $\pm$ SD). (**C**) Brightfield microscopy of samples prepared at different glucose concentrations at 15 min after mixing. Image analysis to quantify (**D**) droplet number and (**E**) droplet diameter at different glucose concentrations, measuring 9 images per sample with n=3 samples/group for both measurements ( $\pm$ SD). (**F**) Confocal laser scanning microscopy for droplets, showing overlay (*left*), FAM-labeled PA-PBA (*middle*), and RhdB-labeled dasiglucagon (*right*). (**G**) TEM of droplets embedded, sectioned using an ultramicrotome, and stained with UranyLess.

PA-PBA at 2 mg/mL is effectively equal in magnitude as the opposing negative charge on dasiglucagon at 0.2 mg/mL. Accordingly, addition of glucose may promote greater charge-balance between the two components, thereby promoting complexation and droplet formation.

To systematically quantify both droplet number and diameter as a function of glucose concentration, microscopy images of droplets prepared in 96-well plates were analyzed with a Python-based automated method (*Fig S3*), collecting nine images per sample with three sample replicates. This analysis confirms negligible droplet formation in the absence of glucose. As glucose level was increased from 25 to 200 mg/dL, the total number of droplets correspondingly increased (*Fig 2D*). Accordingly, droplet formation was highly impacted by glucose concentration. However, the diameter of formed droplets remained relatively constant, in a range of 0.9-1 µm, showing limited impact from glucose concentration (*Fig 2E*).

The highly spherical nature of the resulting droplets supports their existence as a type of coacervate phase, versus a micron-scale aggregate or precipitate.32 The formation of peptide-based droplet phases is an area of increasing interest in the field of drug delivery,33 with several examples of peptide and peptide-polymer hybrid droplets reported thus far. Of note here, PA-PBA is netpositive while dasiglucagon is net-negative. The emergence of a droplet phase through complex coacervation has been reported when (poly)peptides of opposite charges.34,35 The role of glucose in binding to PA-PBA is likewise interesting; glucose binding is seemingly necessary to reduce the extent of positive charge of PA-PBA and ensure effective electrostatic complex formation when mixed with the negatively charged dasiglucagon. Prior work describing glucose-induced peptide droplet formation achieved function through combining a pH-sensitive coacervateforming peptide derived from a type of squid beak with

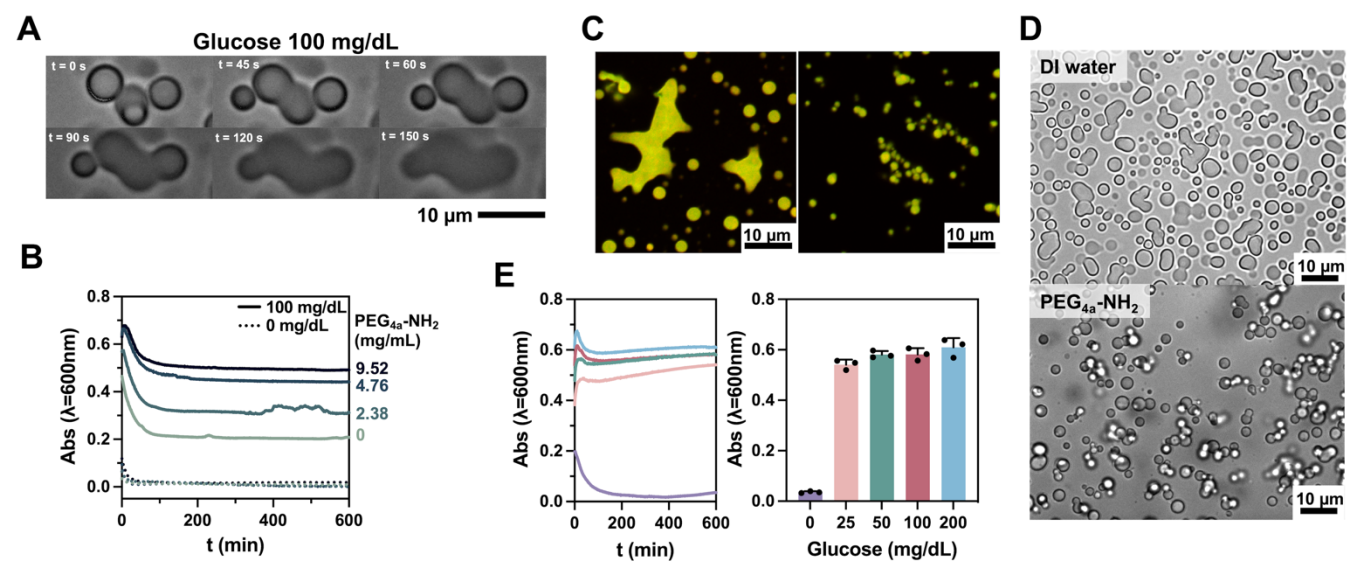


**Figure 3:** (**A**) Brightfield microscopy of PA-PBA and dasiglucagon droplets formed at 100 mg/dL glucose showing fusion over time. (**B**) Turbidity ( $\lambda$ = 600 nm) of droplets prepared at 100 mg/dL glucose or samples at 0 mg/dL glucose and then supplemented 4arm-PEG-NH<sub>2</sub> over a range of polymer concentrations (0-9.52 mg/mL). (**C**) Confocal laser scanning microscopy of droplets 30 min after adding 5 μL DI H<sub>2</sub>O (*left*) or 9.52 mg/mL PEG (*right*). (**D**) Brightfield microscopy at 30 min after adding 5 μL DI H<sub>2</sub>O (*top*) or 9.52 mg/mL PEG (*bottom*). (**E**) Turbidity measurements over time for droplets samples prepared in different glucose concentrations and supplemented with 9.52 mg/mL PEG (*left*), as well as turbidity values compared specifically at 15 min (*right*, n=3/group, ±SD).

glucose oxidase to afford a means of converting glucose level to pH change.<sup>36</sup> Comparatively, the system here offers a direct response to glucose through use of a synthetic binder and droplet formation specifically arises from combination of a PA-based supramolecular material with a therapeutic hormone remedy for dangerously low blood glucose.

Next, to verify that droplets were composed of both PA-PBA and dasiglucagon, PA-PBA was selectively labeled with 5,6-carboxyfluorescein (FAM, Fig S4) and dasiglucagon was labeled with rhodamine B (RhdB, Fig S5). The excitation and emission of these labeled peptides was also verified (Fig S6-S7). FAM-labeled PA-PBA was doped into PA-PBA at 1% of the total PA amount while RhdB-labeled dasiglucagon was doped in at 5% of the total dasiglucagon. After mixing these samples containing labeled constituents in the presence of 100 mg/dL glucose as described above and equilibrating for 15 minutes, confocal laser scanning microscopy (CLSM) was used to image samples (Fig 2F). All droplets showed signals from both FAM and RhdB with complete spatial overlap and homogeneous fluorescence signal within the droplets, supporting formation of a continuous phase rather than an heterogeneous precipitate. Further, these results demonstrate that both PA-PBA and dasiglucagon contribute to droplet formation. Stained TEM was then performed on droplets embedded and sectioned using an ultramicrotome (Fig 2G). These images suggested that the droplets exist as a continuous phase with some subtle texture visible under higher magnification. The form of the underlying nanostructure, and specifically whether PA-PBA forms the originally intended supramolecular fibrils or remains as spherical micelles in the presence of dasiglucagon, is not clear from these images.

2.3 Droplet Interfacial Stabilization. As further evidence of their fluid-like character, droplets were observed to coalesce over short times under observation (Fig 3A). This effect was evident in absorbance data for droplets prepared in the presence of glucose, with a reduction in absorbance corresponding to coalescence over ~1-2 h (Fig 3B). Such behavior is common in LLPS systems with low to moderate surface tension, as the system seeks to minimize its interfacial surface area through droplet fusion.37 In exploring these droplets for applications in therapeutic glucagon delivery, particle instability and rapid fusion are not desirable characteristics. Hydrophilic and amphiphilic polymers have been explored as interfacial stabilizers for their role in enhancing droplet surface tension and preventing coalescence.38,39 Accordingly, the exploration of polymers as interfacial stabilizers was further assessed here.

Various polymers were tested for their role in droplet stabilization. These included a branched polyethylene glycol (PEG, 2 kDa, 4-arm NH<sub>2</sub>-terminated), polyacrylic acid (PAA, 2 kDa) and poly(lactic-co-glycolic)acid (PLGA, 10-50 kDa). For screening purposes, polymer stock solutions (50 mg/mL) were added in a volume of 5  $\mu L$  to a 100  $\mu L$  pre-prepared samples of PA-PBA and dasiglucagon at a glucose concentration of either 0

mg/dL, which did not have droplets, or 100 mg/dL where the droplets were formed and had been allowed to equilibrate for 15 min prior to polymer addition. Absorbance at 600 nm was monitored for these mixtures over time, as before, to determine if the glucose-driven droplet phase was stabilized by the polymer. PAA and PLGA caused an increase in absorbance in the glucosefree case, presumably due to electrostatic interactions and aggregation between these anionic polymers and the netpositive PA-PBA (Fig S8). Accordingly, PAA and PLGA were not further explored here for use in stabilizing these droplets. The branched PEG did not lead to an increase in absorbance in the glucose-free case (Fig S9), indicating no aggregation, and thus behaved comparably to the original mixtures in the absence of glucose. In the presence of 100 mg/dL glucose with addition of branched PEG, the same droplets were observed as before yet the rate of reduction of absorbance due to droplet coalescence was slowed as polymer concentration increased from 0, 2.38, 4.76, and 9.52 mg/mL (Fig 3B). Morphological comparisons of droplets 30 min after addition of branched PEG at 9.52 mg/mL compared to a control diluted with an equivalent volume of water revealed less droplet fusion and improved stability, as observed by CLSM (Fig 3C) and brightfield microscopy (Fig 3D). These studies also revealed likely fusion and spreading onto the glass substrate occurring in the case of the unstabilized droplets. The PEG-stabilized droplets also showed some evidence of glucose-directed increase in droplet formation on the basis of turbidity (Fig 3E), though the glucose-specific differences were not as pronounced as in the case where no PEG stabilizer was added (Fig 2B). The terminal amino groups on the 4-arm PEG-NH2 were critical to droplet stabilization, as a 4-arm PEG-OH of identical molecular weight provided no enhancement in droplet stability (Fig S10). These results suggest electrostatic contributions from the cationic end-groups of the 4-arm PEG-NH2 enable stabilization through association at the droplet interface.

2.4 Droplet Dynamics. Following efforts to prepare stabilized droplets, the dynamics of droplet constituents Fluorescence of interest. recovery photobleaching (FRAP) enables monitoring quantification of molecular diffusion for fluorescently labeled constituents within droplets by photobleaching a region and monitoring fluorescence recovery over time. 40-42 Droplets doped with FAM- and RhdB-labeled constituents were prepared in 100 mg/dL glucose with a 15-minute incubation time, followed by the addition of the 4-arm PEG-NH2 stabilizer. A three-dimensional reconstructed z-stack of the droplets performed via CLSM revealed the existence of a homogenous fluorescent field throughout the droplet for both constituents, pointing to

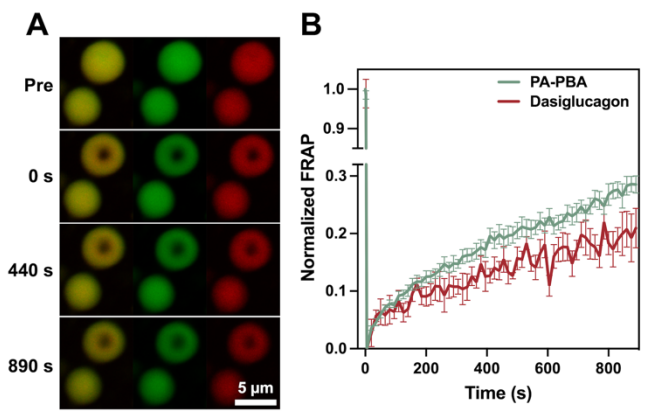


**Figure 4:** (**A**) Fluorescence recovery after photobleaching (FRAP) for droplets showing overlay (*left*), FAM-labeled PA-PBA (*middle*), and RhdB-labeled dasiglucagon (*right*) before bleaching (*Pre*) and then over time after bleaching a region of one droplet. (**B**) Quantification of fluorescence signal in the bleached region of interest for both FAM-labeled PA-PBA and RhdB-labeled dasiglucagon (*n*=3 *samples*, ±*SD*).

a continuous phase and lack of interfacial concentration of either component (Movie S1). The droplet center was then bleached using 488 nm and 561 nm lasers and the fluorescence of the bleached region of interest was monitored for fluorescence recovery. Though recovery was evident for both the PA-PBA (28.5%) and dasiglucagon (25.5%) constituents, in general it was quite limited (Fig 4A,B). The limited volume of the droplet relative to the volume of the region bleached makes complete recovery unlikely, though the bleached region was clearly evident at the endpoint. This result showing slow recovery dynamics supports a more gel-like character of the droplets rather than a highly dynamic liquid-like character; this could be related to the relative size and stability of these PA-PBA-dasiglucagon supramolecular complexes in the context of the time over which diffusion was observed. In related protein-based droplets, structural maturation and interaction of components is similarly known to reduce diffusion within the droplet.17,43,44

**2.5** Functional Dasiglucagon Delivery. To assess the performance of the PA-PBA and dasiglucagon droplets in glucose-directed therapeutic delivery, responsiveness to different glucose levels was further assessed. Droplets were formed at 100 mg/dL glucose in all cases and then incubated in a buffer ranging in glucose level from 0-200 mg/dL. The pre-formed droplets completely dissipated over the course of 60-90 minutes in glucose concentrations of 0 mg/dL and 25 mg/dL (Fig 5A). However, at higher glucose concentrations of 50, 100, and 200 mg/dL, the droplets only exhibited partial dissolution of their structure in this time, with absorbance reduced to

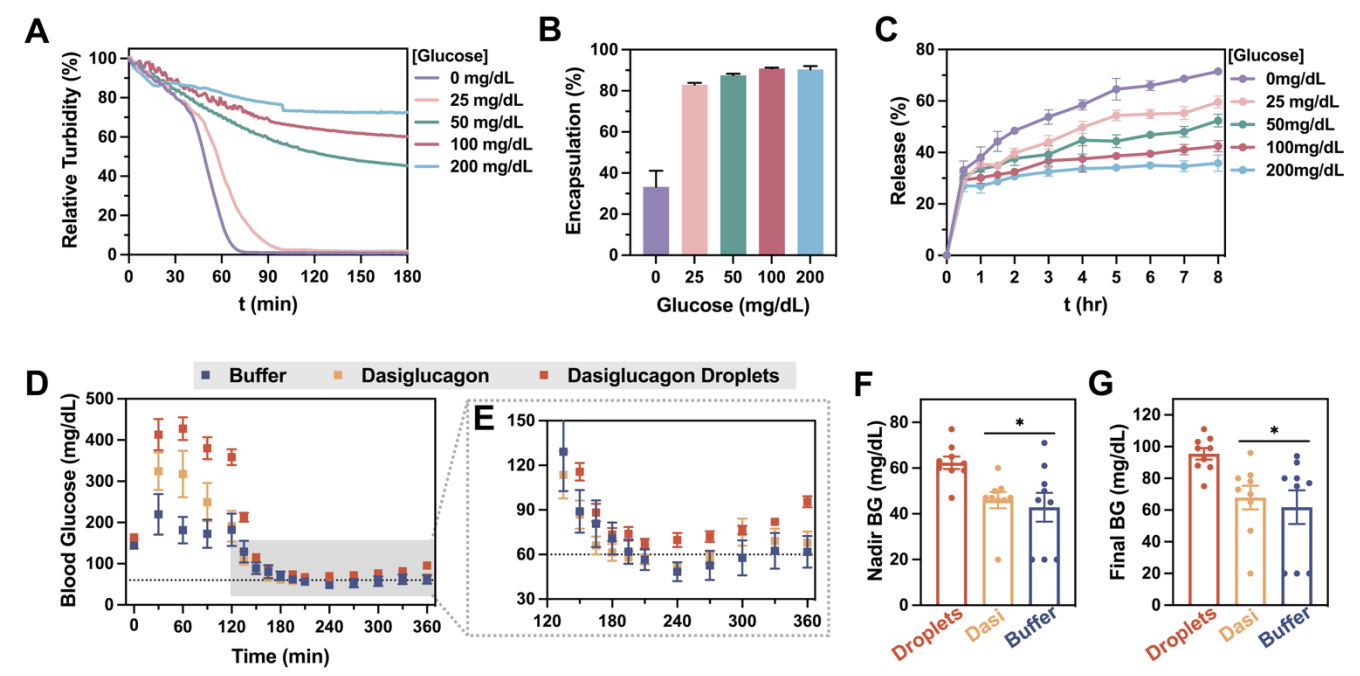


**Figure 5:** (**A**) Change in turbidity over time for droplets prepared at 100 mg/dL glucose and supplemented with 9.52 mg/mL 4arm-PEG-NH<sub>2</sub> before being placed into bulk buffers of different glucose concentrations. (**B**) Encapsulation efficiency determined for PEG-stabilized droplets prepared in different glucose concentrations, determined by measuring the soluble concentration of MCA-labeled dasiglucagon after formation (*n*=3/*group*, ±*SD*). (**C**) Release of MCA-labeled dasiglucagon from droplets prepared at 100 mg/dL glucose and then incubated in bulk buffers of varying glucose concentrations (*n*=3/*group*, ±*SD*). (**D**) A mouse model for prophylactic glucagon delivery prior to severe hypoglycemia was performed, with droplets injected at t=0 min and an insulin overdose administered at t=120 min, monitoring blood glucose throughout and (**E**) specifically focusing on the region of hypoglycemia following insulin overdose. Groups were compared on the basis of (**F**) the lowest (nadir) blood glucose level observed as well as (**G**) the final blood glucose level at 4 h (t = 360 min) after the insulin overdose (n=9/group, ±*SEM*). For panels F and G, data were analyzed by one-way ANOVA and significance (\* - *P*<0.05) is shown for the droplets-treated group compared to the groups treated with dasi or buffer.

45%, 60%, and 72% of its initial values, respectively. Droplet stability was thus enhanced as a function of bulk glucose levels. In order to assess glucose-responsive release of dasiglucagon, a previously reported variant labeled with methylcoumarin (MCA) was used.22 The presence of glucose dramatically increased dasiglucagon encapsulation efficiency, as determined from the amount of dasiglucagon that remained soluble following mixing with PA-PBA (Fig 5B). In agreement with the data on droplet stability, the free dasiglucagon that was released also exhibited an inverse relationship to glucose level (Fig 5C). After 8 h, 80% of glucagon was released from droplets formed at 100 mg/dL glucose and then transferred into a glucose-free bulk; this indicated an improvement in the rate of glucagon release compared to a previously reported PA platform that relied on glucose oxidase for pH-directed hydrogel stability.22

The glucose-stabilized nature of these LLPS droplets was of interest to explore as a glucagon delivery technology in the context of hypoglycemia prevention. A previously established model in STZ-induced diabetic mice simulating prophylactic delivery prior to application of an insulin overdose was employed (*Fig* 5D).<sup>22,28</sup> Following a period of fasting and blood glucose

normalization, droplets prepared in 100 mg/dL glucosecontaining buffer were injected subcutaneously at a total dasiglucagon dose of 6 µg. Controls of buffer or dasiglucagon alone (6 µg) were also administered. Immediately following injection, groups treated with the dasiglucagon droplets or dasiglucagon alone showed an increase in blood glucose. This confirms activity of the therapeutic, but also suggests some extent of undesirable dasiglucagon leakage from the droplets. After 2 h, mice were given an insulin dose of 3 IU/kg to induce hypoglycemia; blood glucose levels following this overdose were more closely inspected (Fig 5E). Specifically, the average nadir (i.e., lowest) value observed in mice (Fig 5F) treated with the LLPS droplets  $(62 \pm 3 \text{ mg/dL})$  was significantly higher than that for mice treated with dasiglucagon alone (46 ± 4 mg/dL) or buffer  $(43 \pm 6 \text{ mg/dL})$ . Mortality offered another measure of the severity of hypoglycemia, with 0% (0/9 mice) dying in the group treated with droplets compared to 11% (1/9) in the group treated with dasiglucagon and 33% (3/9) in the group treated with buffer. The final blood glucose values at 4 h following insulin overdose (Fig 5G) were also significantly higher for mice treated with the LLPS droplets  $(95 \pm 4 \text{ mg/dL})$  compared to that for mice treated with dasiglucagon alone ( $68 \pm 7$  mg/dL) or buffer ( $62 \pm 11$  mg/dL). Overall, the performance of these LLPS droplets in delivering glucagon was comparable to that of the previously reported hydrogel platform using glucose oxidase for glucose sensing in this same animal model.<sup>22</sup> As such, glucose-driven LLPS droplet formation offers function in the delivery of dasiglucagon that may be relevant in the context of a corrective therapeutic strategy to mitigate the effects of hypoglycemia.

#### 3. CONCLUSIONS

The remarkable function from LLPS systems, including membraneless organelles in cell biology, has offered inspiration in designing an array of functional soft materials. A number of bio-inspired synthetic polymers, recombinant proteins, and peptide-based building blocks have been found to demonstrate LLPS phenomena in water. However, in spite of their similarity to natural polymers, there is limited evidence for supramolecular materials participating in LLPS. Herein, the combination of a net-positive peptide amphiphile with a net-negative protein therapeutic, dasiglucagon, underwent LLPS to form gel-like droplets specifically in the presence of glucose. The formation and stability of the droplets here was enhanced under conditions of physiologically relevant glucose concentration. Though the droplets formed upon initial mixture were prone to coalescence, the interface could be stabilized through addition of a hydrophilic branched PEG polymer. Prepared droplets rapidly dissolved when placed into conditions of low glucose, yet remained more stable and dissolved more slowly under conditions of normal to high glucose levels. A therapeutic hormone that corrects low blood glucose, dasiglucagon, was one of the two biomolecular components participating in the complexation driving the initial droplet formation. As such, the observation for both glucose-driven droplet formation and rapid dissolution in the absence of glucose pointed to the possibility of using these droplets for therapeutic delivery of dasiglucagon. These droplets indeed exhibited dasiglucagon release that was reduced on exposure to increased glucose levels, and demonstrated a functional benefit in mitigating the most severe effects of hypoglycemia arising from insulin overdose in a mouse model. Accordingly, beyond reporting an uncommon phenomenon for a supramolecular building block to participate in glucose-driven LLPS and gel-like droplet formation, this current work also points to a functional role for this system in the therapeutic delivery of dasiglucagon toward improved diabetes management.

#### ASSOCIATED CONTENT

# **Supporting Information**

The Supporting Information is available free of charge on the ACS Publications website.

Experimental Methods & Supplemental Data: Microscopy images, image analysis, molecular characterization (.PDF) CLSM Z-Stack Movie (.MOV)

#### **AUTHOR INFORMATION**

## **Corresponding Author**

\* mwebber@nd.edu

#### Notes

The authors declare no competing financial interests.

#### ACKNOWLEDGMENT

We are grateful for technical assistance from the Notre Dame Integrated Imaging Facility (NDIIF) for assistance with TEM (Dr. Maksym Zhukovskyi and Sarah Chapman). MJW gratefully acknowledges funding support for this work from the Helmsley Charitable Trust (2019PG-T1D016 and 2102-04994), the American Diabetes Association Pathway Accelerator Award (1-19-ACE-31), the Juvenile Diabetes Research Foundation (5-CDA-2020-947-A-N), and a National Science Foundation CAREER award (BMAT, 1944875). Schematics in TOC graphic and Fig 1 created using BioRender.com.

## **REFERENCES**

- (1) Shin, Y.; Brangwynne, C. P. Liquid Phase Condensation in Cell Physiology and Disease. *Science* **2017**, *357* (6357). https://doi.org/10.1126/science.aaf4382.
- (2) Hyman, A. A.; Weber, C. A.; Jülicher, F. Liquid-Liquid Phase Separation in Biology. *Annu. Rev. Cell Dev. Biol.* **2014**, *30*, 39–58.
- (3) Hirose, T.; Ninomiya, K.; Nakagawa, S.; Yamazaki, T. A Guide to Membraneless Organelles and Their Various Roles in Gene Regulation. *Nat. Rev. Mol. Cell Biol.* 2022, 24 (4), 288–304.
- (4) Boija, A.; Klein, I. A.; Sabari, B. R.; Dall'Agnese, A.; Coffey, E. L.; Zamudio, A. V.; Li, C. H.; Shrinivas, K.; Manteiga, J. C.; Hannett, N. M.; Abraham, B. J.; Afeyan, L. K.; Guo, Y. E.; Rimel, J. K.; Fant, C. B.; Schuijers, J.; Lee, T. I.; Taatjes, D. J.; Young, R. A. Transcription Factors Activate Genes through the Phase-Separation Capacity of Their Activation Domains. *Cell* 2018, 175 (7), 1842–1855.e16.
- (5) Reinkemeier, C. D.; Girona, G. E.; Lemke, E. A. Designer Membraneless Organelles Enable Codon Reassignment of Selected mRNAs in Eukaryotes. *Science* 2019, 363 (6434). https://doi.org/10.1126/science.aaw2644.
- (6) Garabedian, M. V.; Wang, W.; Dabdoub, J. B.; Tong, M.; Caldwell, R. M.; Benman, W.; Schuster, B. S.; Deiters, A.; Good, M. C. Designer Membraneless Organelles Sequester Native Factors for Control of Cell Behavior. *Nat. Chem. Biol.* 2021, 17 (9), 998–1007.
- (7) Sing, C. E.; Perry, S. L. Recent Progress in the Science of Complex Coacervation. *Soft Matter* **2020**, *16* (12), 2885–2914.
- (8) Yewdall, N. A.; André, A. A. M.; Lu, T.; Spruijt, E. Coacervates as Models of Membraneless Organelles. *Curr. Opin. Colloid*

- Interface Sci. 2021, 52, 101416.
- (9) Liu, J.; Zhorabek, F.; Chau, Y. Biomaterial Design Inspired by Membraneless Organelles. *Matter* **2022**, *5* (9), 2787–2812.
- (10) MacEwan, S. R.; Chilkoti, A. Applications of Elastin-like Polypeptides in Drug Delivery. J. Control. Release 2014, 190, 314– 330.
- (11) Blocher, W. C.; Perry, S. L. Complex Coacervate-Based Materials for Biomedicine. *Wiley Interdiscip. Rev. Nanomed. Nanobiotechnol.* **2017**, 9 (4). https://doi.org/10.1002/wnan.1442.
- (12) Brunsveld, L.; Folmer, B. J.; Meijer, E. W.; Sijbesma, R. P. Supramolecular Polymers. Chem. Rev. 2001, 101 (12), 4071–4098.
- (13) Hartgerink, J. D.; Beniash, E.; Stupp, S. I. Peptide-Amphiphile Nanofibers: A Versatile Scaffold for the Preparation of Self-Assembling Materials. *Proc. Natl. Acad. Sci. U. S. A.* 2002, 99 (8), 5133–5138.
- (14) Hartgerink, J. D.; Beniash, E.; Stupp, S. I. Self-Assembly and Mineralization of Peptide-Amphiphile Nanofibers. *Science* 2001, 294 (5547), 1684–1688.
- (15) Cui, H.; Webber, M. J.; Stupp, S. I. Self-Assembly of Peptide Amphiphiles: From Molecules to Nanostructures to Biomaterials. *Biopolymers* **2010**, *94* (1), 1–18.
- (16) Webber, M. J.; Pashuck, E. T. (Macro)molecular Self-Assembly for Hydrogel Drug Delivery. Adv. Drug Deliv. Rev. 2021, 172, 275–295.
- (17) Kanaan, N. M.; Hamel, C.; Grabinski, T.; Combs, B. Liquid-Liquid Phase Separation Induces Pathogenic Tau Conformations in Vitro. Nat. Commun. 2020, 11 (1), 2809.
- (18) Ma, L.; Fang, X.; Wang, C. Peptide-Based Coacervates in Therapeutic Applications. Front Bioeng Biotechnol 2022, 10, 1100365.
- (19) Xiang, Y.; Su, B.; Liu, D.; Webber, M. J. Managing Diabetes with Hydrogel Drug Delivery. Adv. Ther. 2023. https://doi.org/10.1002/adtp.202300127.
- (20) Hendricks, M. P.; Sato, K.; Palmer, L. C.; Stupp, S. I. Supramolecular Assembly of Peptide Amphiphiles. Acc. Chem. Res. 2017. https://doi.org/10.1021/acs.accounts.7b00297.
- (21) Webber, M. J.; Berns, E. J.; Stupp, S. I. Supramolecular Nanofibers of Peptide Amphiphiles for Medicine. *Isr. J. Chem.* **2013**, *53* (8), 530–554.
- (22) Yu, S.; Xian, S.; Ye, Z.; Pramudya, I.; Webber, M. J. Glucose-Fueled Peptide Assembly: Glucagon Delivery via Enzymatic Actuation. *J. Am. Chem. Soc.* **2021**, *143* (32), 12578–12589.
- (23) Marco-Dufort, B.; Tibbitt, M. W. Design of Moldable Hydrogels for Biomedical Applications Using Dynamic Covalent Boronic Esters. *Materials Today Chemistry* 2019, 12, 16–33.
- (24) Kitano, S.; Hisamitsu, I.; Koyama, Y.; Kataoka, K.; Okano, T.; Sakurai, Y. Effect of the Incorporation of Amino Groups in a Glucose-Responsive Polymer Complex Having Phenylboronic Acid Moieties. *Polym. Adv. Technol.* 1991, 2 (5), 261–264.
- (25) Shiino, D.; Kubo, A.; Murata, Y.; Koyama, Y.; Kataoka, K.; Kikuchi, A.; Sakurai, Y.; Okano, T. Amine Effect on Phenylboronic Acid Complex with Glucose under Physiological pH in Aqueous Solution. J. Biomater. Sci. Polym. Ed. 1996, 7 (8), 697–705.
- (26) Greenfield, M. A.; Hoffman, J. R.; de la Cruz, M. O.; Stupp, S. I. Tunable Mechanics of Peptide Nanofiber Gels. *Langmuir* 2010, 26 (5), 3641–3647.
- (27) Stendahl, J. C.; Rao, M. S.; Guler, M. O.; Stupp, S. I. Intermolecular Forces in the Self-Assembly of Peptide Amphiphile Nanofibers. Adv. Funct. Mater. 2006, 16 (4), 499–508.
- (28) Yu, S.; Ye, Z.; Roy, R.; Sonani, R. R.; Pramudya, I.; Xian, S.; Xiang, Y.; Liu, G.; Flores, B.; Nativ-Roth, E.; Bitton, R.; Egelman, E. H.; Webber, M. J. Glucose-triggered Gelation of Supramolecular Peptide Nanocoils with Glucose-binding

- Motifs. *Adv. Mater.* **2023**. https://doi.org/10.1002/adma.202311498.
- (29) Hövelmann, U.; Bysted, B. V.; Mouritzen, U.; Macchi, F.; Lamers, D.; Kronshage, B.; Møller, D. V.; Heise, T. Pharmacokinetic and Pharmacodynamic Characteristics of Dasiglucagon, a Novel Soluble and Stable Glucagon Analog. *Diabetes Care* 2018, 41 (3), 531–537.
- (30) Rajangam, K.; Behanna, H. A.; Hui, M. J.; Han, X.; Hulvat, J. F.; Lomasney, J. W.; Stupp, S. I. Heparin Binding Nanostructures to Promote Growth of Blood Vessels. *Nano Lett.* 2006, 6 (9), 2086– 2090.
- (31) Ghanaati, S.; Webber, M. J.; Unger, R. E.; Orth, C.; Hulvat, J. F.; Kiehna, S. E.; Barbeck, M.; Rasic, A.; Stupp, S. I.; Kirkpatrick, C. J. Dynamic in Vivo Biocompatibility of Angiogenic Peptide Amphiphile Nanofibers. *Biomaterials* 2009, 30 (31), 6202–6212.
- (32) Cakmak, F. P.; Choi, S.; Meyer, M. O.; Bevilacqua, P. C.; Keating, C. D. Prebiotically-Relevant Low Polyion Multivalency Can Improve Functionality of Membraneless Compartments. *Nat. Commun.* 2020, 11 (1), 5949.
- (33) Liu, J.; Spruijt, E.; Miserez, A.; Langer, R. Peptide-Based Liquid Droplets as Emerging Delivery Vehicles. *Nature Reviews Materials* **2023**, *8* (3), 139–141.
- (34) Priftis, D.; Tirrell, M. Phase Behaviour and Complex Coacervation of Aqueous Polypeptide Solutions. Soft Matter 2012, 8 (36), 9396–9405.
- (35) Abbas, M.; Lipiński, W. P.; Wang, J.; Spruijt, E. Peptide-Based Coacervates as Biomimetic Protocells. *Chem. Soc. Rev.* 2021, 50 (6), 3690–3705.
- (36) Lim, Z. W.; Ping, Y.; Miserez, A. Glucose-Responsive Peptide Coacervates with High Encapsulation Efficiency for Controlled Release of Insulin. *Bioconjug. Chem.* 2018. https://doi.org/10.1021/acs.bioconjchem.8b00369.
- (37) Titus, A. R.; Ferreira, L. A.; Belgovskiy, A. I.; Kooijman, E. E.; Mann, E. K.; Mann, J. A., Jr; Meyer, W. V.; Smart, A. E.; Uversky, V. N.; Zaslavsky, B. Y. Interfacial Tension and Mechanism of Liquid-Liquid Phase Separation in Aqueous Media. *Phys. Chem. Chem. Phys.* 2020, 22 (8), 4574–4580.
- (38) Park, S.; Barnes, R.; Lin, Y.; Jeon, B.-J.; Najafi, S.; Delaney, K. T.; Fredrickson, G. H.; Shea, J.-E.; Hwang, D. S.; Han, S. Dehydration Entropy Drives Liquid-Liquid Phase Separation by Molecular Crowding. *Commun Chem* **2020**, *3* (1), 83.
- (39) Mason, A. F.; Buddingh', B. C.; Williams, D. S.; van Hest, J. C. M. Hierarchical Self-Assembly of a Copolymer-Stabilized Coacervate Protocell. J. Am. Chem. Soc. 2017, 139 (48), 17309–17312.
- (40) Muzzopappa, F.; Hummert, J.; Anfossi, M.; Tashev, S. A.; Herten, D.-P.; Erdel, F. Detecting and Quantifying Liquid-Liquid Phase Separation in Living Cells by Model-Free Calibrated Half-Bleaching. *Nat. Commun.* 2022, 13 (1), 7787.
- (41) Taylor, N. O.; Wei, M.-T.; Stone, H. A.; Brangwynne, C. P. Quantifying Dynamics in Phase-Separated Condensates Using Fluorescence Recovery after Photobleaching. *Biophys. J.* **2019**, 117 (7), 1285–1300.
- (42) Boeynaems, S.; De Decker, M.; Tompa, P.; Van Den Bosch, L. Arginine-Rich Peptides Can Actively Mediate Liquid-Liquid Phase Separation. *Bio Protoc* 2017, 7 (17), e2525.
- (43) Ashami, K.; Falk, A. S.; Hurd, C.; Garg, S.; Cervantes, S. A.; Rawat, A.; Siemer, A. B. Droplet and Fibril Formation of the Functional Amyloid Orb2. *J. Biol. Chem.* **2021**, 297 (1), 100804.
- (44) Babinchak, W. M.; Surewicz, W. K. Liquid-Liquid Phase Separation and Its Mechanistic Role in Pathological Protein Aggregation. J. Mol. Biol. 2020, 432 (7), 1910–1925.